

# New Nematic LCD with Submillisecond Response Time

Haiwei Chen,<sup>1</sup> Yuge Huang,<sup>1</sup> Fangwang Gou,<sup>1</sup> Javed Rouf Talukder,<sup>1</sup> Ming-Chun Li,<sup>2</sup> Seok-Lyul Lee,<sup>2</sup> and Shin-Tson Wu<sup>1</sup>

<sup>1</sup>College of Optics and Photonics, University of Central Florida, Orlando, Florida 32816, USA

<sup>2</sup> AU Optronics Corp., Hsinchu 30078, Taiwan

## Abstract

We report a new vertical alignment fringe in-plane switching (VA-FIS) liquid crystal device with single alignment on top substrate. This design exhibits submillisecond response time, reasonably high transmittance (~70%), and relatively low operation voltage (15 V). It is a strong contender for next-generation field sequential color displays.

## Keywords

Liquid crystal display; Fast response; Field sequential color displays.

## 1. Introduction

Field sequential color (FSC) liquid crystal display (LCD) is a strong contender for next-generation display technology, as it exhibits two major advantages: 3x higher resolution density and 3x higher optical efficiency [1-3]. These two features are highly desirable for high-end TVs and emerging augmented reality and vertical reality displays. However, to suppress the color breakup of FSC LCDs, the required response time should be less than 1 ms [4-6]. This imposes a big challenge to LCD because its response time is usually in the order of 10 ms [7, 8].

To achieve submillisecond response time, polymer-stabilized short-pitch cholesteric liquid crystal (e.g. blue phase, uniform standing helix, or uniform lying helix) is an effective approach [9]. However, the operation voltage for such LC modes is still too high [10], and the driving scheme is also complicated [11]. For example, to operate a polymer-stabilized blue phase LCD, 3-4 thin-film transistors (TFTs) per pixel are required to compensate the slow charging time [12]. Another option to get sub-millisecond response is the so-called triode structure [13, 14]. It uses an erasing field to accelerate the LC relaxation process. In experiment, a response time of ~0.1 ms has been demonstrated. But still, the bottleneck is the demanding TFT driving circuit [14].

Recently, a vertical alignment fringe in-plane switching (VA-FIS) mode was proposed and fast response was obtained even at -30°C [15]. Its driving scheme is simple and the TFT charging time is fast, but the trade-offs are twofold: increased voltage and decreased transmittance. In this paper, we modify this VA-FIS structure by removing the bottom alignment layer. This important step significantly increases the transmittance and lowers the operation voltage. Meanwhile, both rise time and decay time are less than 1 ms. To achieve good dark state, we can apply a small bias voltage to the common electrode of the bottom substrate.

## 2. Device structure

Figure 1 depicts the schematic diagram of our proposed top-alignment VA-FIS mode. As the name implies, only top substrate has surface alignment, which induces vertical alignment at the voltage-off state. The employed LC has a positive dielectric anisotropy ( $\Delta\epsilon > 0$ ). Meanwhile, on the top substrate there is a planar electrode with a bias voltage ( $V_{\text{bias}}$ ). Combined with bottom common electrode ( $V_{\text{com}} = 0$ ), a strong vertical electric field is produced in the whole panel. This vertical field plays two important roles: 1) The LC directors are vertically aligned along

the electric field with suppressed thermal fluctuation, leading to a high contrast ratio, and 2) the LC directors are forced to return to their initial state when the horizontal electric field is removed, leading to a fast decay time.

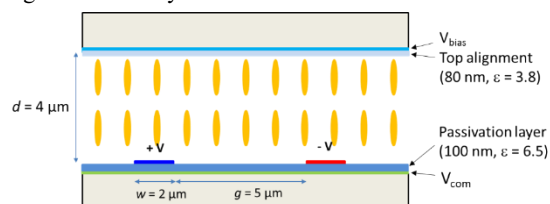


**Figure 1.** Schematic diagram of the proposed top-alignment VA-FIS mode.

On the bottom substrate, the interdigitated pixel electrodes and common electrode are separated by a passivation layer. Please note that for pixel electrodes, the applied voltages have different polarities. Thus, the strength of horizontal electric field is doubled. This structure is called fringe in-plane switching (FIS) mode, since both fringe field and in-plane field coexist [16]. However, it requires 2 TFTs so that the aperture ratio is reduced slightly.

## 3. Simulation results

The electro-optic properties of our VA-FIS mode are calculated by a commercial LCD simulator DIMOS.2D and the extended Jones matrix [17]. The cell parameters are: electrode width  $w = 2 \mu\text{m}$ , electrode gap  $g = 5 \mu\text{m}$ , and cell gap  $d = 4 \mu\text{m}$ . A 100-nm-thick  $\text{Si}_3\text{N}_4$  (dielectric constant  $\epsilon = 6.5$ ) is employed as the passivation layer. The LC material used here is a positive  $\Delta\epsilon$  LC material with low rotational viscosity [18, 19]. Its physical properties are:  $K_{11} = 12.7 \text{ pN}$ ,  $K_{22} = 6.4 \text{ pN}$ ,  $K_{33} = 14.0 \text{ pN}$ ,  $\Delta n = 0.125$ ,  $\Delta\epsilon = 6.7$ , and  $\gamma_1 = 53 \text{ mPas}$ . Also, a bias voltage ( $V_{\text{bias}} = 4 \text{ V}$ ) is applied to the top electrode to generate vertical electric field.

### 3.1 Electro-optic effects

Firstly, we investigate conventional VA-FIS with alignment on both substrates. Fig. 2 shows the simulated results (black lines) of voltage-dependent transmittance (VT) and time-dependent transmittance (tT) curves. The response time is indeed quite fast [rise time: 1.07 ms, decay time: 0.61 ms]. However, from Fig. 2(a), the on-state voltage is higher than 20 V and the transmittance at 15 V is only 58%, which is too low for practical applications.

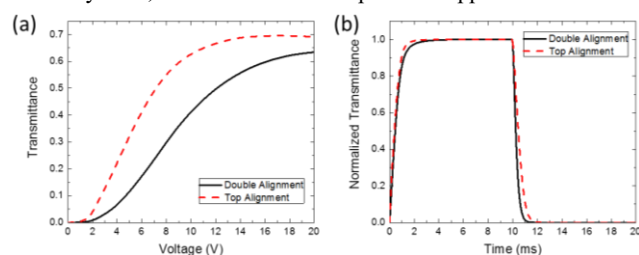


**Figure 2.** Simulated (a) VT and (b) tT curves for VA-FIS with and without bottom alignment layer.  $\lambda = 550 \text{ nm}$ .

On the other hand, our proposed top-alignment VA-FIS mode shows significant improvement in comparison to the double-alignment VA-FIS LCD. For example, as shown in Fig. 12(a), the VT curve of the top-alignment VA-FIS increases much earlier and faster. Further, the corresponding on-state voltage is only 17 V, and transmittance at 15 V is as high as 69.3%. Moreover, as listed in Table 1, sub-millisecond response time is realized for both rise time and decay time (rise time: 0.91 ms, decay time: 0.93 ms). This is highly desirable for FSC LCDs, to suppress the annoying color break-up issue.

**Table 1. Simulated VA-FIS device performance of different alignment conditions.**

	$V_{on}$	T @ 15 V	Rise time	Decay time
Double alignment	> 20 V	58.0%	1.07 ms	0.61 ms
Top alignment	15 V	69.3%	0.91 ms	0.93 ms
Bottom alignment	> 20 V	58.7%	1.14 ms	0.62 ms
No alignment	15.4 V	66.5%	1.05 ms	0.95 ms

To better understand the underlying physical mechanism, we compare the LC director distributions for both modes: double-side alignment and top alignment. Results are plotted in Fig. 3(a) and 3(b), respectively. Clearly, for the double-side alignment [Fig. 3(a)], the LC directors near bottom substrate stand still due to strong anchoring force. But for the top-alignment [Fig. 3(b)], these LC molecules in the same area rotate freely and easily along the electric field. As a result, the phase retardation is larger and required voltage is lower.

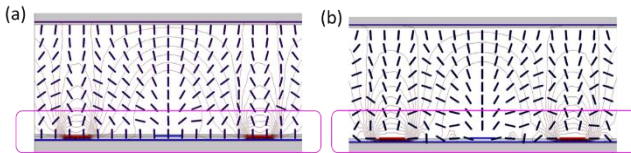


**Figure 3.** Simulated LC director distribution for (a) VA-FIS with double-side alignment, and (b) VA-FIS with top alignment.

**3.2 Different alignment conditions**

Next, we investigate two more alignment conditions: 1) single alignment layer on the bottom substrate, and 2) no alignment layer on both substrates. Results are shown in Fig. 4, and data are summarized in Table 1.

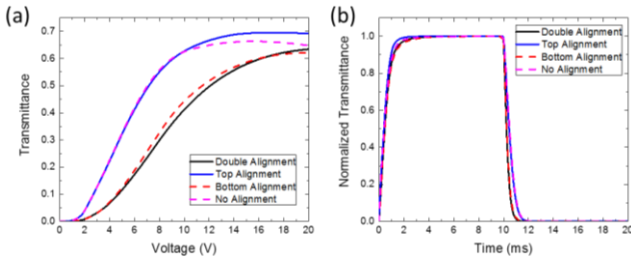


**Figure 4.** Simulated (a) VT and (b) tT curves for different alignment conditions. (Double alignment: two alignment layers; top alignment: one alignment layer on top substrate; bottom alignment: one alignment layer on bottom substrate; no alignment: no alignment on either substrate)

Interestingly, the bottom-alignment case shows similar performance to that of double-alignment, although the top alignment layer is removed. This is because the LC molecular reorientations mainly happen near the bottom substrate (with FIS electrodes), which are governed by the bottom alignment layer. Then as expected, once we remove this bottom alignment layer,

the device performance would be improved noticeably, as the top-alignment case (blue line) and no-alignment case (magenta line) shown in Fig. 4.

**3.3 Bias voltage effect**

The bias voltage on the top electrode is a key factor affecting the device performance. Here, we increase this voltage from 3 V to 5 V, and results are shown in Fig. 5. As expected, when the bias voltage increases, the response time decreases dramatically because the vertical electric field becomes stronger. But the on-state voltage becomes higher (e.g., 14 V to 20 V), and the transmittance becomes lower (e.g., 70.4% to 65.8% at 15 V). To balance all the desired performances,  $V_{bias} = 4$  V is a good choice.

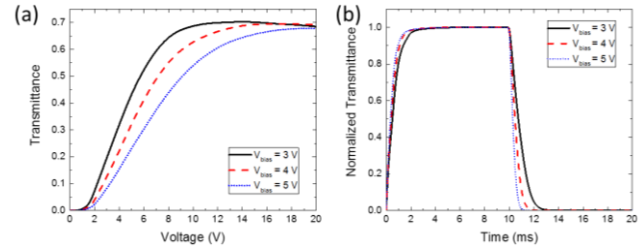


**Figure 5.** Simulated (a) VT and (b) tT curves for different bias voltages.

**3.4 Passivation layer effect**

For conventional fringe field switching (FFS) mode, the passivation layer should be as thin as possible to mitigate the voltage shielding effect and lower the operation voltage. But in VA-FIS, it is different. As depicted in Fig. 6, when the passivation layer gets thicker, the operation voltage becomes lower, e.g.  $V_{on} = 9.6$  V for  $t_{pass} = 0.5$   $\mu\text{m}$ . This is because in the VA-FIS structure, two forces are competing each other: vertical electric field and horizontal electric field. For a thick passivation layer, the corresponding vertical electric field becomes weaker. As a result, the horizontal electric field would dominate and the LC directors would be reoriented more easily, leading to a much lower  $V_{on}$ .

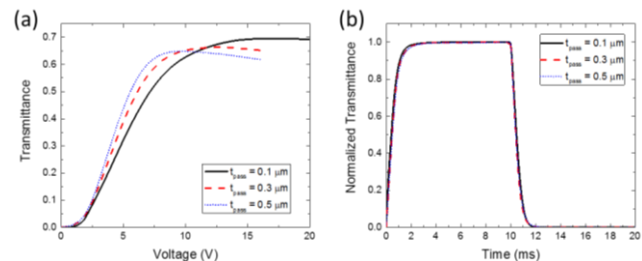


**Figure 6.** Simulated (a) VT and (b) tT curves for different passivation layer thicknesses.

**3.5 Degraded dark state**

As discussed above, increasing the passivation layer thickness seems to be a viable option to reduce the operation voltage. But unexpectedly, the dark state and threshold voltage are sacrificed, as shown in Fig. 7. In conventional VA-FIS with double-side alignment, no bias voltage is used (black line). As a result, it shows the best dark state with a certain threshold voltage to prevent the light leakage resulted from TFT instability. When a biased voltage of 4 V is applied (red line), threshold voltage is greatly decreased. This is because the LC alignment is already perturbed by the vertical electric field, thus, a relatively weak horizontal electric field can reorient the LC directors. Similarly, for the top-alignment

VA-FIS cell we proposed, its threshold voltage is also reduced significantly, especially as the passivation layer thickness increases (blue, magenta, and green curves).

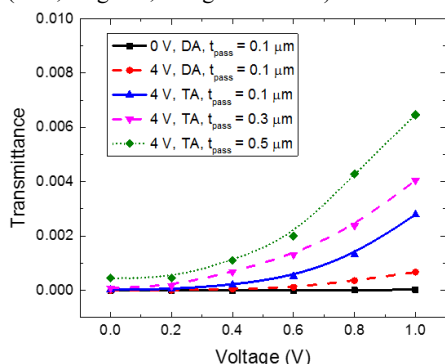


**Figure 7.** Simulated dark state and threshold voltage for different thicknesses of passivation layer. (DA: double alignment; TA: top alignment)

This effect can be visualized more clearly in Fig. 8. For the double-alignment without a bias voltage [Fig. 8(a)], no vertical field exists and the LCs are well aligned, showing an outstanding dark state. When a bias voltage is present [Fig. 8(b)], in theory, the electric field should be vertical. However, it is not perfectly vertical due to voltage shielding effect of passivation layer. As shown in Fig. 8(b), electric field is slanted. In this case, some LC directors are already reoriented, so that the threshold behavior is smeared. If we further remove the bottom alignment and increase the passivation layer thickness [Figs. 8(c) - 8(e)], this effect is more obvious.

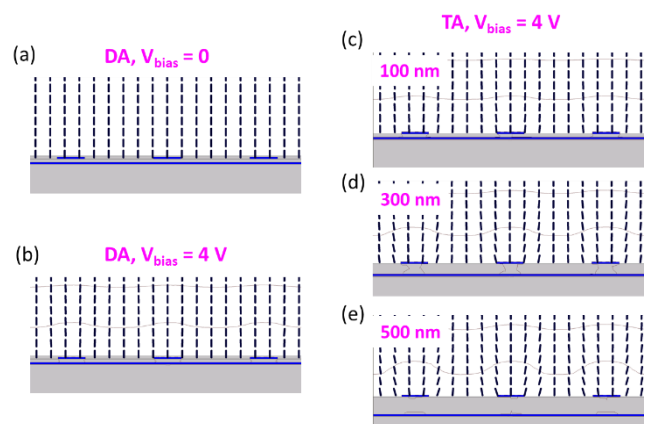


**Figure 8.** Simulated LC director and equipotential line distribution for (a) double alignment without bias voltage; (b) double alignment with a bias voltage; (c) – (e) top alignment with 100 nm, 300 nm, and 500 nm thick passivation layer. All the top alignment cases have a 4 V bias voltage.

**3.6 Common voltage effect**

To overcome the aforementioned light leakage issue, we could apply a small bias voltage to the bottom common electrode. As shown in Fig. 9(b), when  $V_{com}$  is -0.8 V, it compensates the voltage shielding of passivation layer almost perfectly, leading to a much uniform electric field. As a result, a better dark state and threshold behavior is recovered, as plotted in Fig. 9(c).

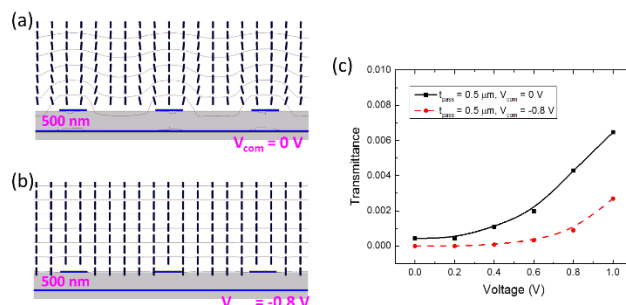


**Figure 9.** Simulated LC director and equipotential line distribution for top-alignment VA-FIS with (a)  $V_{com} = 0$  V; (b)  $V_{com} = -0.8$  V; and (c) simulated dark state and threshold voltage for these two conditions. (The thickness of passivation layer is 500 nm.  $V_{bias} = 4$  V)

**4. Discussion**

**4.1 Anchoring energy effect**

For the above discussions, we focus on the top-alignment condition, where bottom alignment layer is totally removed. But for some cases, bottom alignment layer is still preferred in order to keep good vertical alignment for achieving a high contrast ratio. With such motivation, we carry out more investigations on the anchoring energy effect. Results are plotted in Fig. 10. If the anchoring energy is weak ( $W = 10^{-6} \sim 10^{-5}$  N/m), it performs almost the same as that of zero anchoring energy. This means the bottom alignment layer is not necessarily removed, as long as its anchoring energy is weak. As the anchoring energy increases ( $W = 10^{-3} \sim 10^{-2}$  N/m), the on-state voltage increases while transmittance decreases.

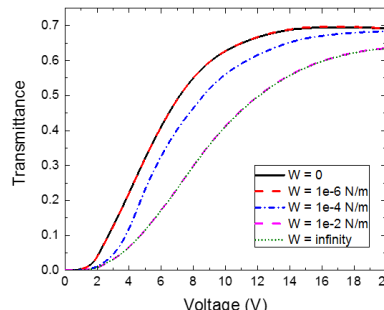


**Figure 10.** Simulated VT curves for different anchoring energies of bottom substrate. (Top alignment is fixed with strong anchoring energy)

**4.2 Gray-to-gray response time**

Table 2 shows the simulated gray-to-gray (GTG) response time. Here, we divided the VT curve into 256 gray levels based on Gamma-2.2 rule. As usual, the response time between any two gray levels is defined by 10% to 90% transmittance change.

**Table 2. Simulated GTG response time of top-alignment VA-FIS mode with  $V_{bias} = 4$  V.**

Voltage	0 V	1.87 V	3.27 V	5.55 V	15 V
Gray Level	1	64	128	192	256
1		2.43	2.53	3.57	0.91
64	0.39		1.66	1.73	0.64
128	0.56	1.32		1.87	0.51
192	0.78	1.25	1.69		0.38
256	0.93	1.14	1.58	1.27	

From Table 2, the average GTG response time is 1.36 ms. If the display is driven at 120 fps, the corresponding GTG motion picture response time (MPRT) is 6.80 ms. If the backlight is modulated at 20% duty ratio [20], then the average GTG MPRT is reduced to 1.90 ms. In most cases, the motion image blur is at indistinguishable level [21, 22].

#### 4.2 Viewing angle

For single-domain VA, its viewing angle property is quite limited, as shown in Fig. 11(a). To improve that, compensation films and zigzag electrode configuration are commonly practiced. Here, we choose a positive A-plate, a negative C-plate and a negative A-plate for VA-FIS compensation [23]. The obtained isocontrast contour is plotted in Fig. 11(b). It is clearly seen the compensated viewing angle is widened significantly. The contrast ratio over 200:1 is expanded to  $\sim 70^\circ$  viewing cone.

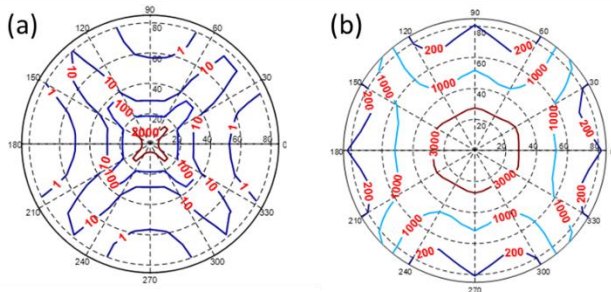


**Figure 11.** Viewing-angle performance of top-alignment VA-FIS mode (a) single-domain without compensation films and (b) multi-domain with +A, -C, -A compensation films. ( $\lambda = 550$  nm)

#### 5. Conclusion

We have proposed a novel top-alignment VA-FIS mode to achieve submillisecond response time while keeping a reasonably high transmittance ( $T \sim 70\%$ ) and low operation voltage ( $V = 15$  V). A potential concern is the degraded dark state and much reduced threshold voltage due to non-uniform vertical electric field. To improve that, we propose to apply a small bias voltage to the bottom common electrode to compensate the voltage shielding effect from the passivation layer. Good performance is obtained. We believe this design would have widespread applications for next-generation FSC LCDs.

#### References

- [1] T. Takahashi, H. Furue, M. Shikada, et al. "Preliminary study of field sequential fullcolor liquid crystal display using polymer stabilized ferroelectric liquid crystal display," *Jpn. J. Appl. Phys.* **38**(5A), L534-L536 (1999).
- [2] F. Peng, F. Gou, H. Chen, et al. "A submillisecond-response liquid crystal for color sequential projection displays," *J. Soc. Inf. Disp.* **24**(4), 241-245 (2016).
- [3] H. Chen, J. H. Lee, B. Y. Lin, et al. "Liquid crystal display and organic light-emitting diode display: present status and future perspectives," *Light Sci. Appl.* **7**, e17168 (2018).
- [4] F. C. Lin, Y. P. Huang, C. M. Wei, et al. "Color-breakup suppression and low-power consumption by using the Stencil-FSC method in field-sequential LCDs," *J. Soc. Inf. Disp.* **17**(3), 221-228 (2009).
- [5] H. Chen, F. Gou, and S. T. Wu, "A submillisecond-response nematic liquid crystal for augmented reality displays," *Opt. Mater. Express* **7**(1), 195-201 (2017).
- [6] F. Gou, H. Chen, M. C. Li, et al. "Submillisecond-response liquid crystal for high-resolution virtual reality displays," *Opt. Express* **25**(7), 7984-7997 (2017).
- [7] M. Schadt, "Milestone in the history of field-effect liquid crystal displays and materials," *Jpn. J. Appl. Phys.* **48**, 03B001 (2009).
- [8] H. Chen, Z. Luo, D. Xu, et al. "A fast-response A-film-enhanced fringe field switching liquid crystal display," *Liq. Cryst.* **42**(4), 537-542 (2015).
- [9] G. Tan, Y. H. Lee, F. Gou, et al. "Review on polymer-stabilized short-pitch cholesteric liquid crystal displays," *J. Phys. D: Appl. Phys.* **50**, 493001 (2017).
- [10] H. Chen, Y. F. Lan, C. Y. Tsai, et al. "Low-voltage blue-phase liquid crystal display with diamond-shape electrodes," *Liq. Cryst.* **44**(7), 1124-1130 (2017).
- [11] Y. Huang, H. Chen, G. Tan, et al. "Optimized blue-phase liquid crystal for field-sequential-color displays," *Opt. Mater. Express* **7**(2), 641-650 (2017).
- [12] C. L. Lin, M. H. Cheng, C. D. Tu, et al. "Design of pixel circuits for blue-phase liquid crystal displays," *J. Display Technol.* **12**(2), 153-157 (2016).
- [13] D. J. Channin, "Triode optical gate: A new liquid crystal electro-optic device," *Appl. Phys. Lett.* **26**(11), 603-605 (1975).
- [14] D. Xu, H. Chen, S. T. Wu, et al. "A fringe field switching liquid crystal display with fast grayscale response time," *J. Display Technol.* **11**(4), 353-359 (2015).
- [15] Y. Iwata, M. Murata, K. Tanaka, et al. "Novel super fast response vertical alignment-liquid crystal display with extremely wide temperature range," *J. Soc. Inf. Disp.* **22**(1), 35-42 (2014).
- [16] J. W. Park, Y. J. Ahn, J. H. Junh, et al. "Liquid crystal display using combined fringe and in-plane electric fields," *Appl. Phys. Lett.* **93**(8), 081103 (2008).
- [17] A. Lien, "Extended Jones matrix representation for the twisted nematic liquid-crystal display at oblique incidence," *Appl. Phys. Lett.* **57**(26), 2767-2769 (1990).
- [18] H. Chen, F. Peng, Z. Luo, et al. "High performance liquid crystal displays with a low dielectric constant material," *Opt. Mater. Express* **4**(11), 2262-2273 (2014).
- [19] H. Chen, M. Hu, F. Peng, et al. "Ultra-low viscosity liquid crystals," *Opt. Mater. Express* **5**(3), 655-660 (2015).
- [20] J. I. Hirakata, A. Shingai, Y. Tanaka, et al. "Super-TFT-LCD for moving picture images with the blink backlight system," *SID Symp. Dig. Tech. Paper* **32**(1), 990-993 (2001).
- [21] H. Chen, F. Peng, F. Gou, et al. "Nematic LCD with motion picture response time comparable to organic LEDs," *Optica* **3**(9), 1033-1034 (2016).
- [22] F. Peng, H. Chen, F. Gou, et al. "Analytical equation for the motion picture response time of display devices," *J. Appl. Phys.* **121**(2), 023108 (2017).
- [23] X. Zhu, Z. Ge, and S. T. Wu, "Analytical solutions for uniaxial-film-compensated wide-view liquid crystal displays," *J. Display Technol.* **2**(1), 2-20 (2006).